THE INFLUENCE OF B_θ ON INJECTION AND TRANSPORT IN A TOROIDAL OCTUPOLE MAGNETIC FIELD

J. C. Sprott

November 1966

PLP 84
Copy No. 55

University of Wisconsin
Thermonuclear Plasma Studies

THE INFLUENCE OF B_θ ON INJECTION AND TRANSPORT IN A TOROIDAL OCTUPOLE MAGNETIC FIELD*

(Presented at November 1966 Boston Meeting of the Div. of Plasma Physics American Physical Soc.)

J. C. Sprott

ABSTRACT

A tenuous 40 eV hydrogen plasma is injected into the Wisconsin toroidal octupole[1] from outside the magnetic field. The plasma polarizes upon entering the field and $\vec{E} \times \vec{B}$ drifts toward the low field region where the plasma encounters the same field lines again but in the opposite direction, discharging the polarization field. The plasma then splits into two clouds which $\vec{E} \times \vec{B}$ drift around the machine by producing an octupole electric field. The addition of an azimuthal field, B_θ, causing a 35° azimuthal pitch for the spiraling field lines near the wall, did not appreciably reduce the amount of plasma transported, nor did it inhibit the transport around the machine, in spite of the fact that the clouds travelling in opposite directions require octupole electric fields of opposite polarity. There was some tendency for

*Work supported by the U. S. Atomic Energy Commission

[1] R. A. Dory, D. W. Kerst, D. M. Meade, W. E. Wilson and C. W. Erickson, Phys. Fluids 9, 997 (1966).

the competing fields to cancel one another, but for the most part, potential gradients along magnetic field lines were sufficiently large to allow the plasma to move around the machine. Some plasma was also observed to travel around the center of the machine moving parallel to B_θ field lines.

INTRODUCTION

When an azimuthal magnetic field is added to a toroidal octupole, the theories of injection and transport encounter several difficulties. It might be conjectured that plasma injected from outside the magnetic field would continue across the field colliding with the opposite wall. Furthermore, if the plasma did stop near the minimum field point and split into two clouds, they would have difficulty moving around the toroid because of the short circuiting effect of the spiraling field lines. In fact, both of these effects have been observed, but neither occurs to a sufficient extent to appreciably reduce the trapping efficiency. After plasma has uniformly filled the machine, the number of particles trapped with B_θ is at most 10% smaller than without B_θ. To understand how B_θ changes things, we must first review the theory of injection into an octupole with closed field lines.

EXPERIMENTAL

Figure 1 shows a slab of plasma entering the octupole field. The magnetic field is generated by

the induced currents in four copper rods which give a downward field of about 1 kilogauss at the outside wall. The entering positive ions are deflected to the left by the field, while the electrons are deflected to the right creating a polarization electric field with a magnitude just sufficient to allow the entering plasma to $\vec{E} \times \vec{B}$ drift across the field with its free flight velocity of 1.2×10^7 cm/sec. As the plasma continues inward, it encounters the same field lines again but in the opposite direction. This time, a polarization electric field cannot develop because of the good conductivity parallel to field lines. The plasma is brought to an abrupt halt near the zero field point and spreads out azimuthally. When B_θ is added, the field lines no longer close on themselves but spiral around the hoops. If the pitch of the spiral is sufficiently large, it might not be possible for the short circuiting to take place and the plasma would not be stopped. In our case, the pitch was small, and the plasma was stopped as is indicated in Figure 2.

Floating potential measurements were made with special attenuated probes[2] which could reliably measure frequencies up to 10 MHz with densities as low as $10^7 cm^{-3}$. Since the electron temperature was small and reasonably constant, electric fields were assumed to be given by the gradient of the floating potential. The upper curves

---

[2] J. C. Sprott, RSI, 37, 897 (1966).

in Figure 2 show the floating potential across the horizontal midplane at the injection port 14 μsec after the gun fires. The large positive potential near the inside wall is caused by a small number of ions overshooting their associated electrons as the plasma is brought to a halt. When B_θ is added, the profile moves in a few centimeters implying that plasma penetrates slightly farther across the field. The lower curves are scans along the vertical midplane at the injection port. The significant feature here is the electric field which develops in the middle when B_θ is added. Its value is such as to give an $\vec{E} \times \vec{B}$ drift of about 4×10^6 cm/sec toward the inner wall. This is about one third of its initial velocity, which means that the plasma has nearly come to rest by the time it reaches the center.

When the plasma stops, it splits into two approximately equal clouds which move around the toroid perpendicular to the magnetic field. Figure 3 shows the octupole electric fields which are generated by the moving plasma in the absence of B_θ. To a very good approximation, the magnetic field lines are equipotentials. Potential measurements during transport show a peak negative potential at $\psi = +0.5$ and a positive peak at $\psi = -3.5$. The walls and rods are at zero potential. With $B_\theta = 0$, the electric field is everywhere orthogonal to the magnetic field and gives an $\vec{E} \times \vec{B}$ drift which is in the same direction as the

bulk velocity in the center of the machine and in the opposite direction in the cross-hatched areas near the wall and near the rods.

The time evolution of the moving plasma can be seen by measuring the time dependence of potentials as a function of ψ. Figure 4 shows the result. Equipotential surfaces are plotted as a function of ψ and time for a scan between a rod and the wall. These contours propagate to the left with a nearly constant velocity. Although equipotential lines are not flow lines in the laboratory system, a transformation to the moving frame does not change the general character of the potentials, but only moves the circulation centers inward. The plasma density peaks near the middle several μsec behind the circulation centers. Most of the plasma is moving forward with only a few high velocity particles participating in the circulation. This double vortex motion has been predicted theoretically[3] and has been observed in other experiments.[4,5]

The plasma cloud on the opposite side of the injection port is moving in the opposite direction with respect to the magnetic field and hence it generates an electric field with reversed polarity. No difficulty arises as long as

---

[3] J. W. Poukey, to be published in Phys.Fluids

[4] W. H. Bostick, Proc. of Symposium on Electromagnetics and Fluid Dynamics of Gaseous Plasmas. Ed. by J. Fox (Polytechnic Press, Brooklyn, N. Y. 1962) p 211

[5] G. O. Barney, Bull. Am. Phys. Soc. 11, 452 (1966).

the field lines are in a constant θ plane, but when B_θ is added, the field lines spiral around the machine and tend to short out the electric fields. If the short circuiting were perfect, plasma could not $\vec{E} \times \vec{B}$ drift around the toroid. Figure 5 shows the influence of B_θ on the octupole electric fields on each side of the injection port. The curves at the left show the lower half of the octupole electric fields at + and - 50° from the injection port in the absence of B_θ. When B_θ is added, the potentials are distorted because of the short circuiting effect. Potential measurements during transport were difficult because of the shot-to-shot irreproducibility, which was worse with the azimuthal field present. Each of the data points represents an average of three shots.

A direct attempt was made to measure the potential drop parallel to the field by placing two probes on the same field line as it makes one spiral across the injection port. The result is shown in Figure 6. The potential difference between the two points in the absence of B_θ is plotted for comparison. When B_θ is added, the potential difference decreases but fields of greater than 100 volts/meter parallel to $\vec{B}$ are still observed. This potential gradient is believed fact that plasma has not had ample time to fill in the

regions behind the rods. By 17 μsec the potential difference has fallen to zero, but by that time, most of the plasma has already moved past the probes.

Density measurements were also made with a special biased double probe[2] which had a frequency response of 1 MHz. Figure 7 shows contours of equal density across the horizontal midplane at $\theta = +50°$ with full B_θ. One peak is observed toward the outside wall and another at the middle where the field is purely azimuthal. The earlier peak is moving by $\vec{E} \times \vec{B}$ drift across the field, while the other is drifting parallel to the field lines. When B_θ is removed, the density peak at the center does not appear. On the opposite side of the injection port, the situation is reversed with one peak toward the inside wall and another at the center, as shown in Figure 8. The contours in Figures 7 and 8 are in units of $10^{10} cm^{-3}$.

All of these data were obtained using the maximum value of B_θ which was available. The azimuthal field was 260 gauss or about 1/4 as large as the multipole field at the outside wall in the midplane. Smaller values of B_θ showed a gradual transition from the zero B_θ to the full B_θ case. Reversing the direction of B_θ produced no appreciable change in injection or transport.

In summary, it can be said that to a first approxi-

mation, the plasma flows azimuthally, creating whatever electric fields it requires to do so, while the short circuited magnetic field lines distort the flow only slightly.

ACKNOWLEDGMENT

The author expresses appreciation to J. A. Berryman for much helpful assistance in data compilation.

FIGURES

1. Theory of Injection Process

2. Potentials at Injection Port

3. Octupole Field Showing Direction of $\vec{E} \times \vec{B}$

4. Equipotential Surfaces at Rod Port

5. Influence of B_θ on Octupole Electric Fields

6. Potential Drop Across Injection Port

7. Equal Density Surfaces at Port 8 with B_θ

8. Equal Density Surfaces at Port 2 with B_θ

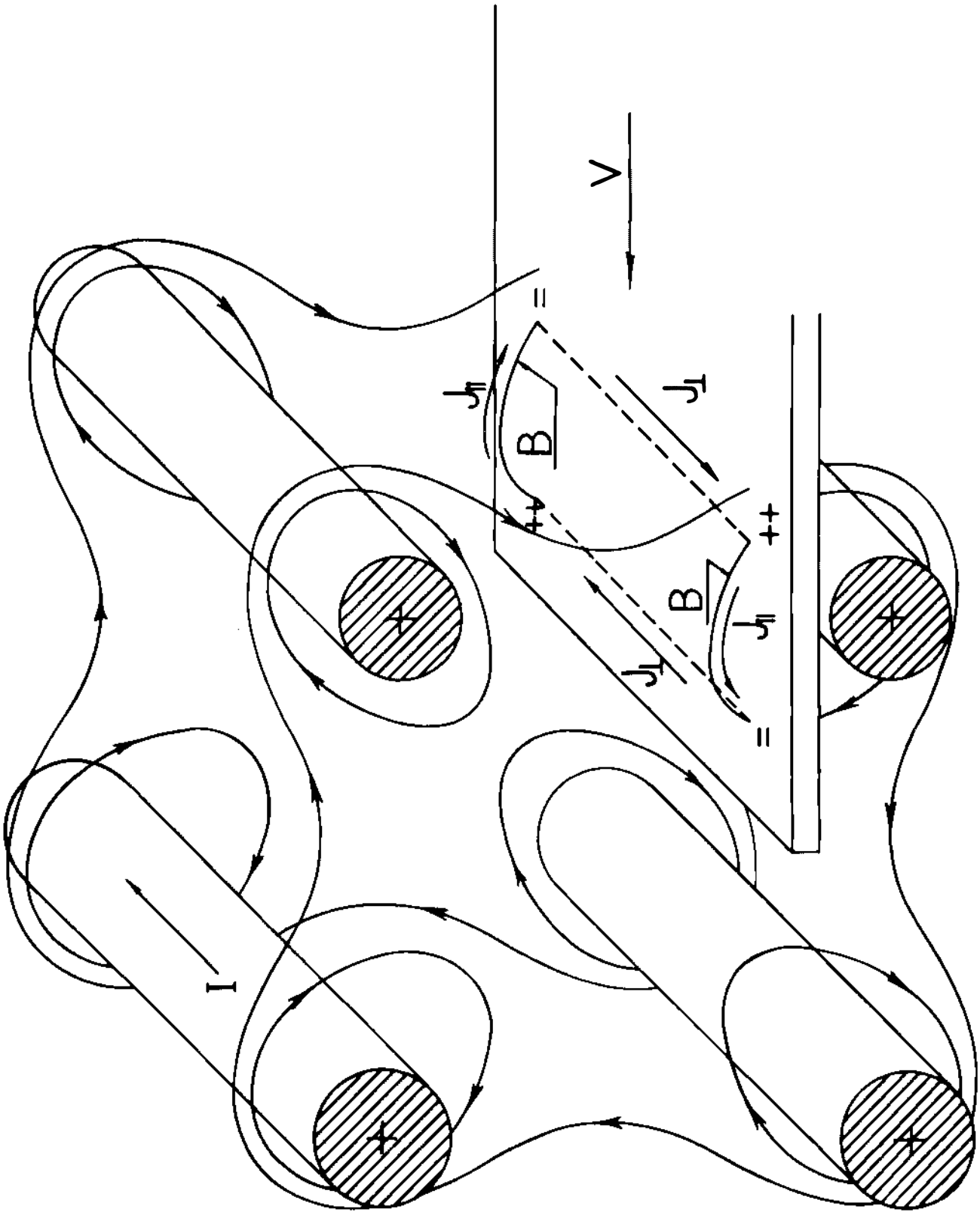

Figure 1

INFLUENCE OF B_θ ON INJECTION PORT POTENTIALS

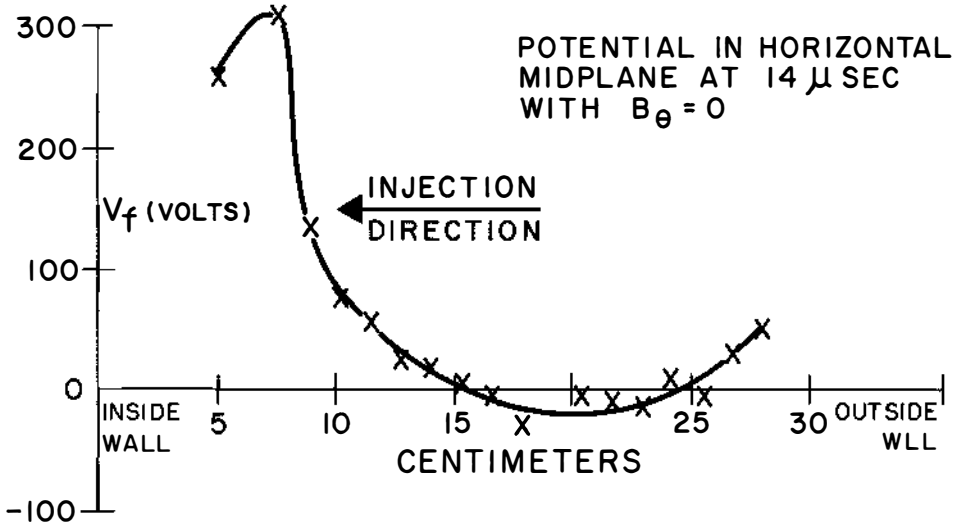

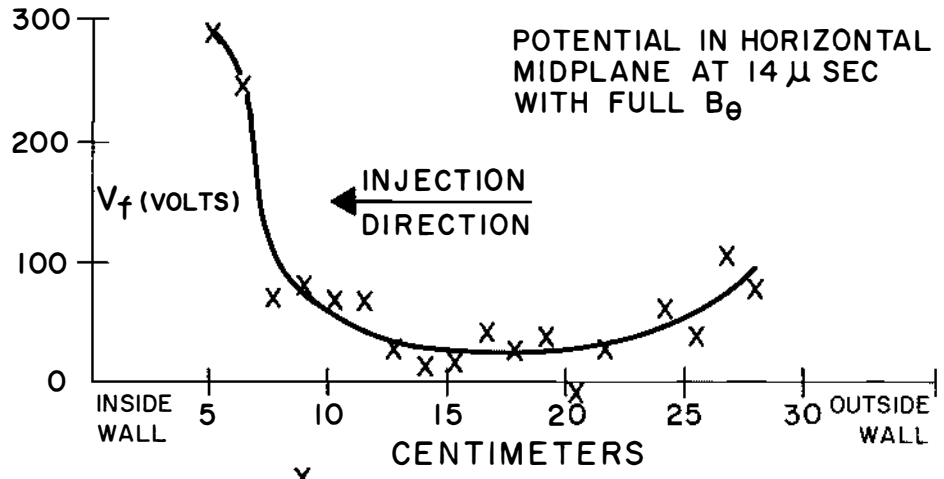

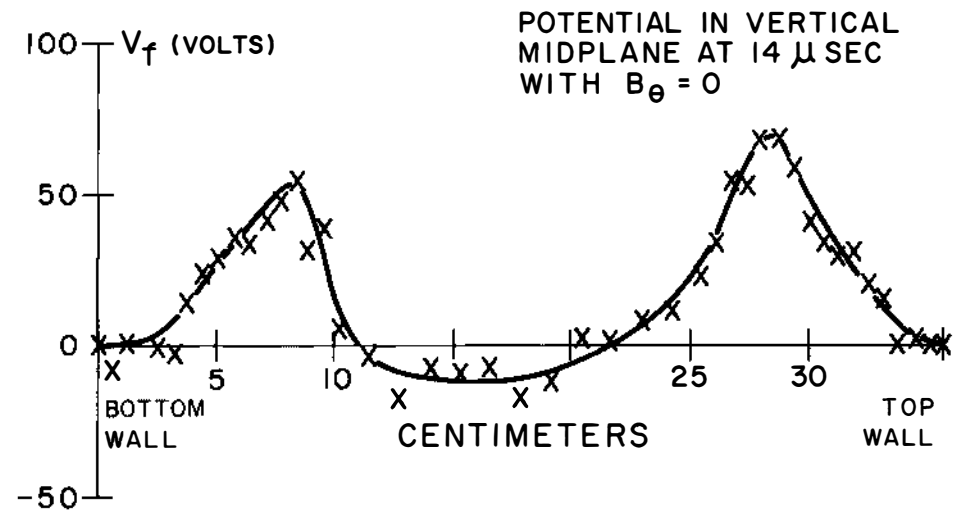

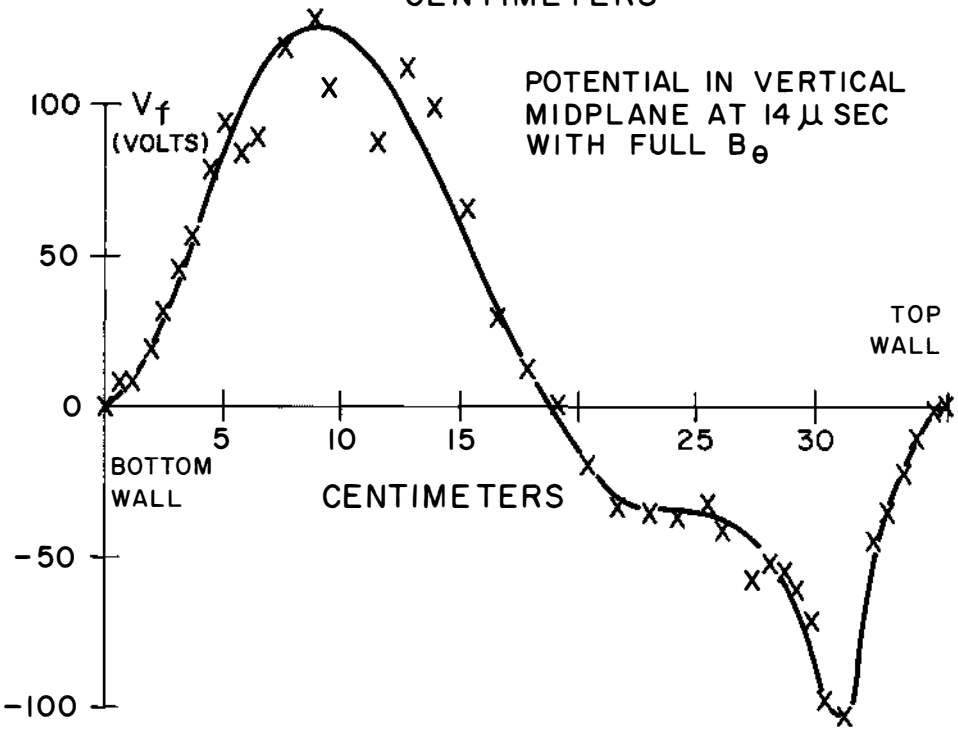

Figure 2

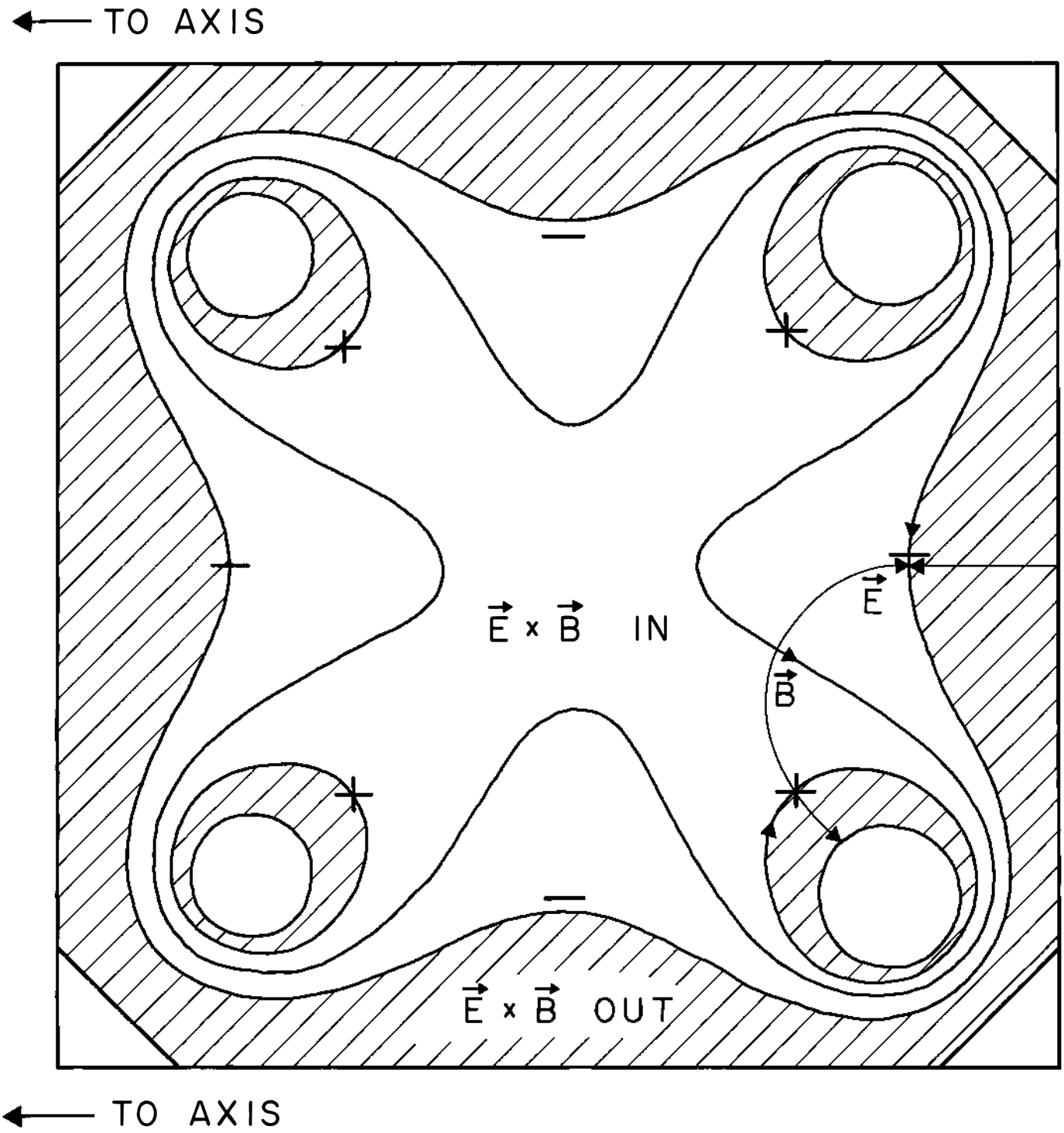

CROSS SECTION OF TOROIDAL OCTUPOLE MAGNETIC FIELD SHOWING DIRECTION OF $\vec{E} \times \vec{B}$ DRIFT VELOCITY

Figure 3

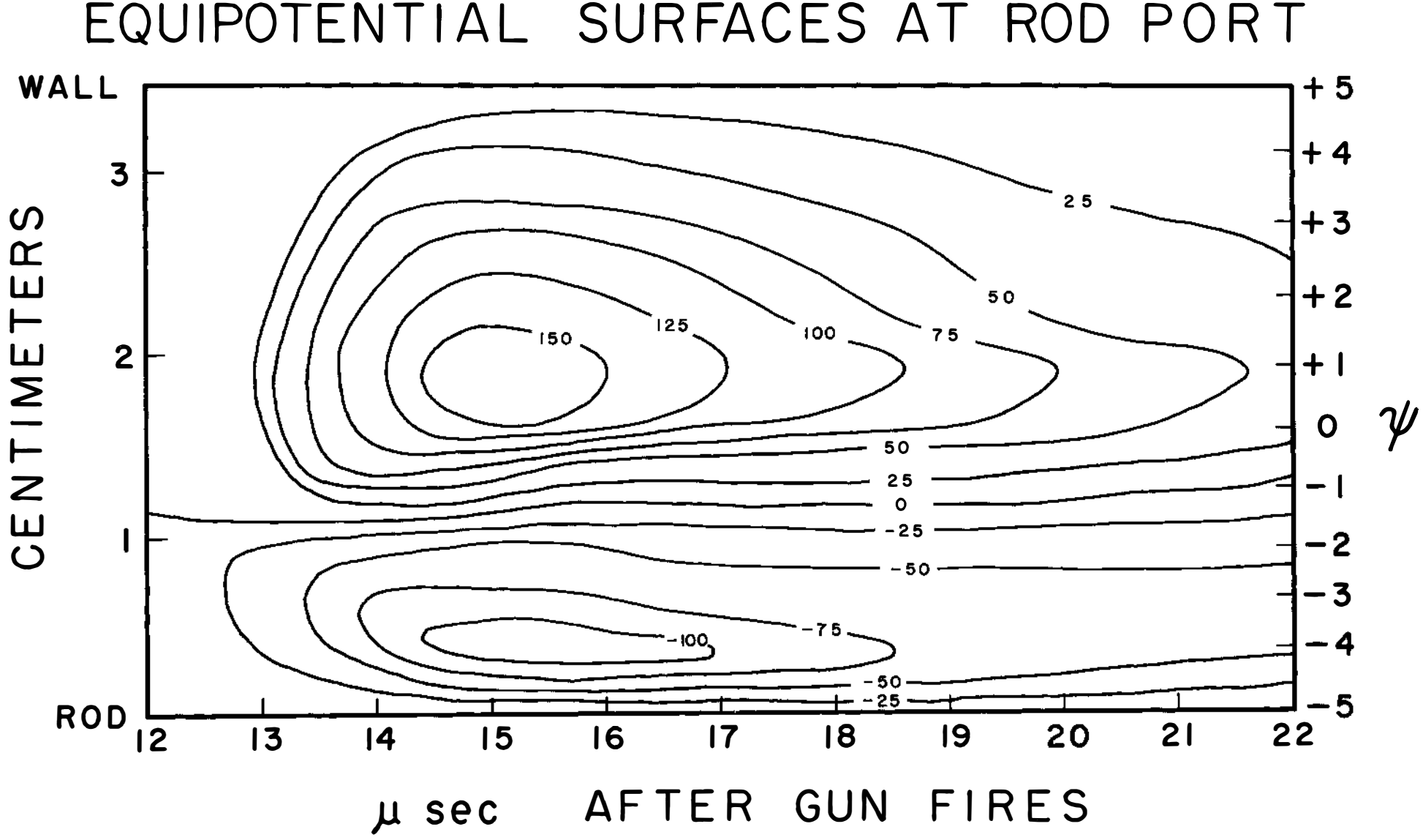
EQUIPOTENTIAL SURFACES AT ROD PORT
WALL
ROD
CENTIMETERS
3
2
1
+5
+4
+3
+2
+1
0
−1
−2
−3
−4
−5
ψ
25
50
75
100
125
150
50
25
0
−25
−50
−75
−100
−50
−25
12
13
14
15
16
17
18
19
20
21
22
μ sec AFTER GUN FIRES

Figure 4

INFLUENCE OF B_θ ON OCTUPOLE ELECTRIC FIELDS

SCANS ARE AT ρ = 10CM AND 14 μ SEC

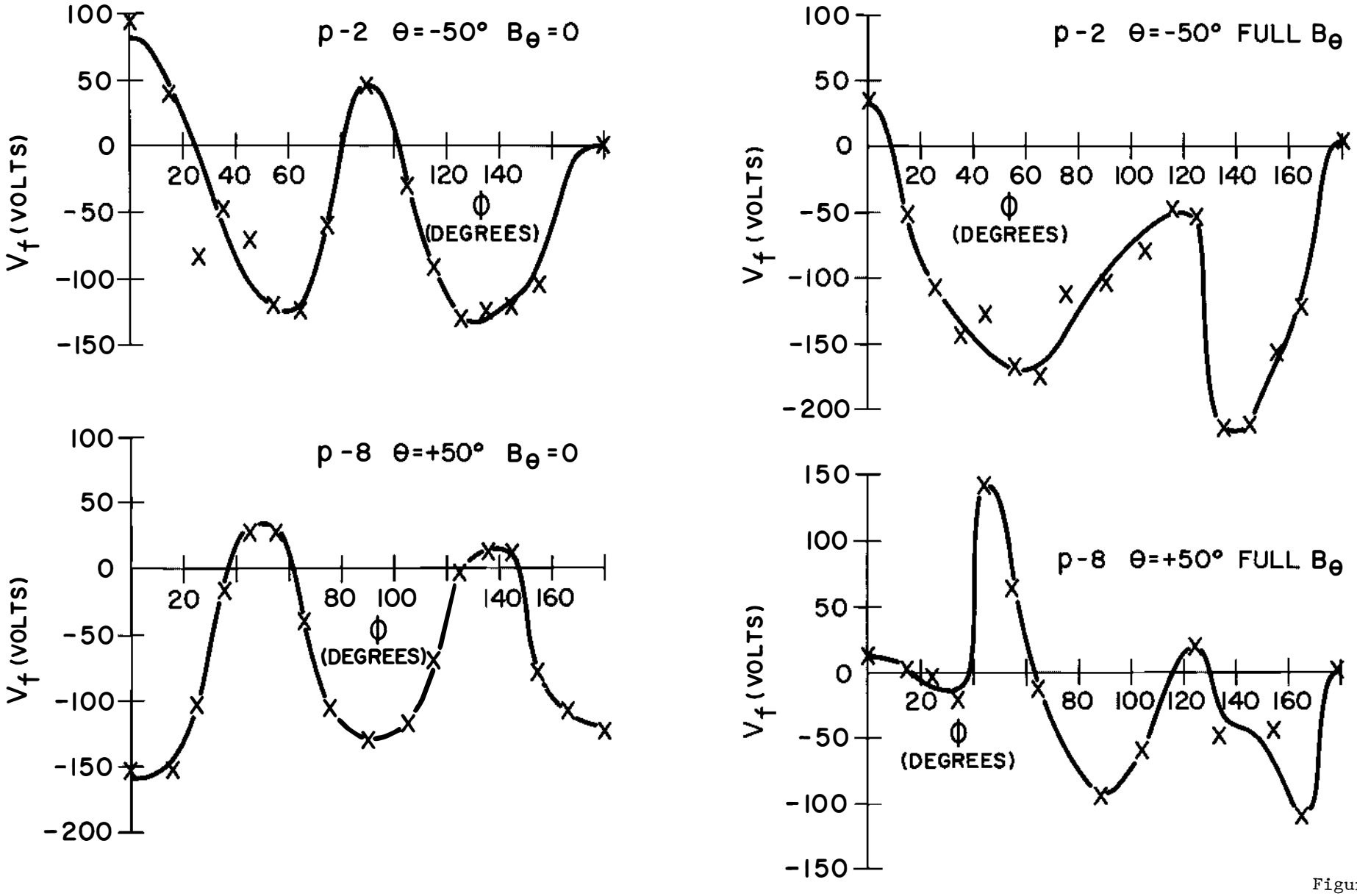

Figure 5

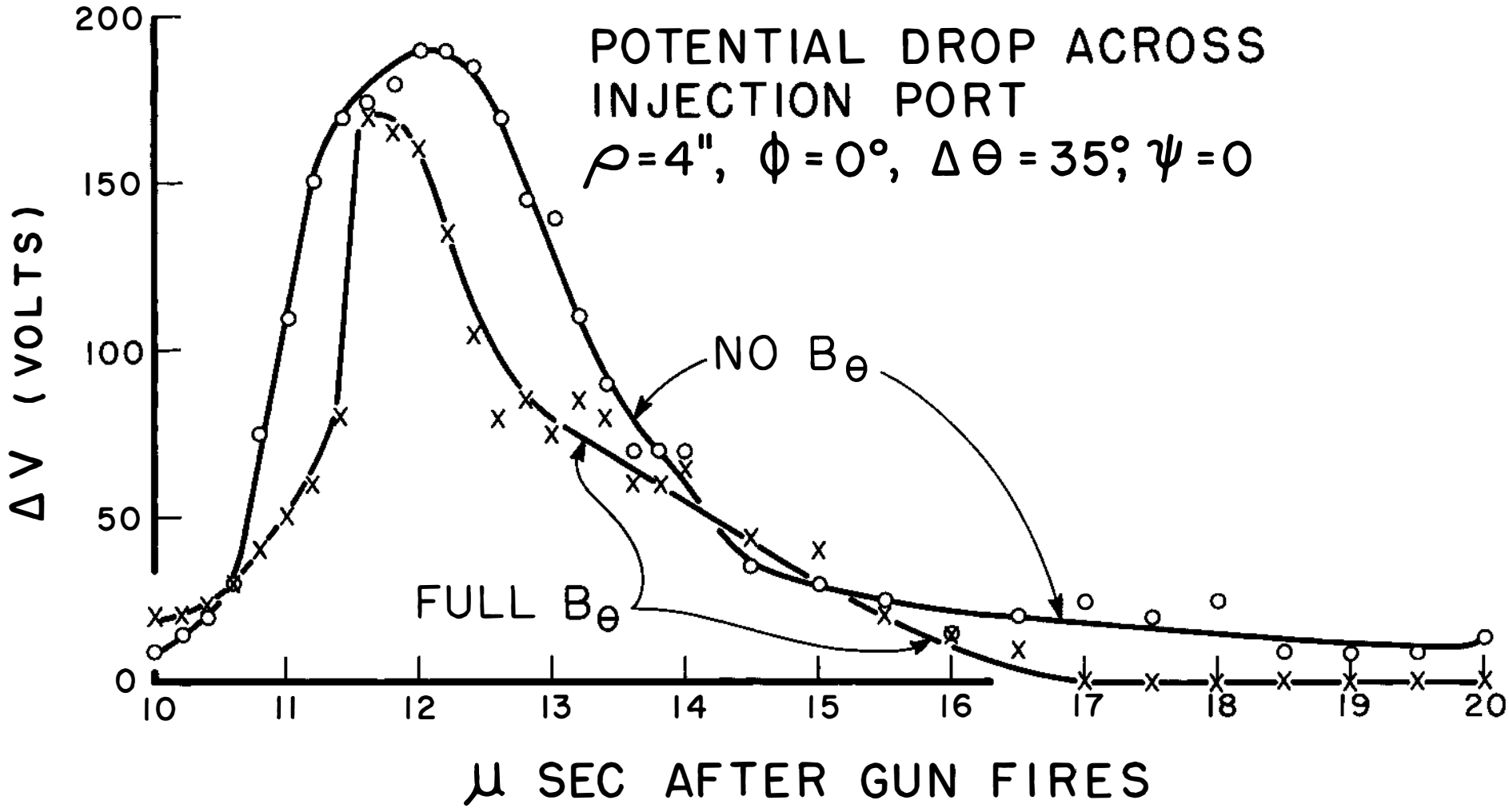
POTENTIAL DROP ACROSS
INJECTION PORT
ρ=4", Φ=0°, ΔΘ=35°, ψ=0
NO Bθ
FULL Bθ
ΔV (VOLTS)
200
150
100
50
0
10
11
12
13
14
15
16
17
18
19
20
μ SEC AFTER GUN FIRES

Figure 6

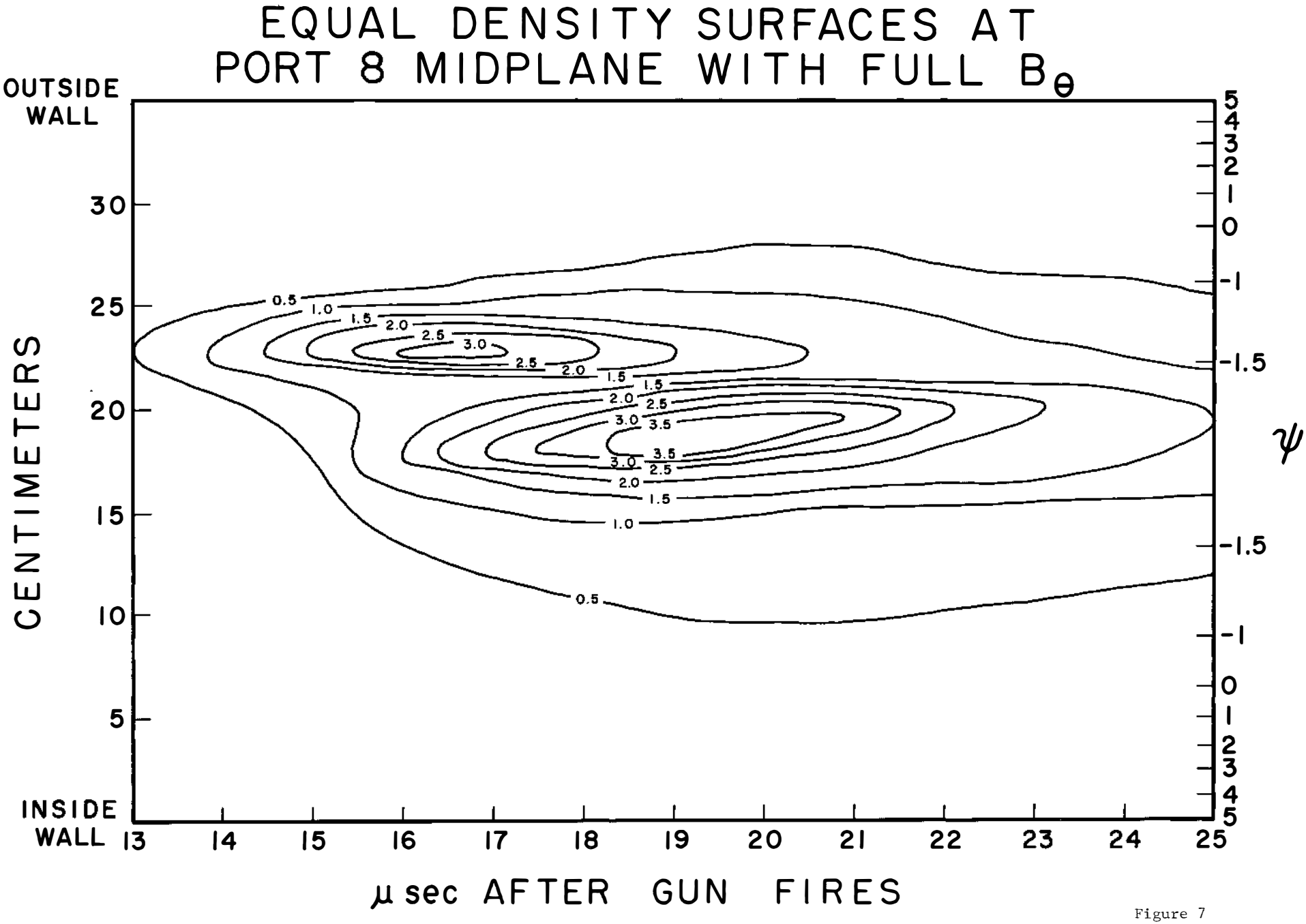
EQUAL DENSITY SURFACES AT
PORT 8 MIDPLANE WITH FULL B_θ
OUTSIDE WALL
INSIDE WALL
CENTIMETERS
30
25
20
15
10
5
0.5
1.0
1.5
2.0
2.5
3.0
3.5
13
14
15
16
17
18
19
20
21
22
23
24
25
μ sec AFTER GUN FIRES
5
4
3
2
1
0
-1
-1.5
-1.5
-1
0
1
2
3
4
5
ψ

Figure 7

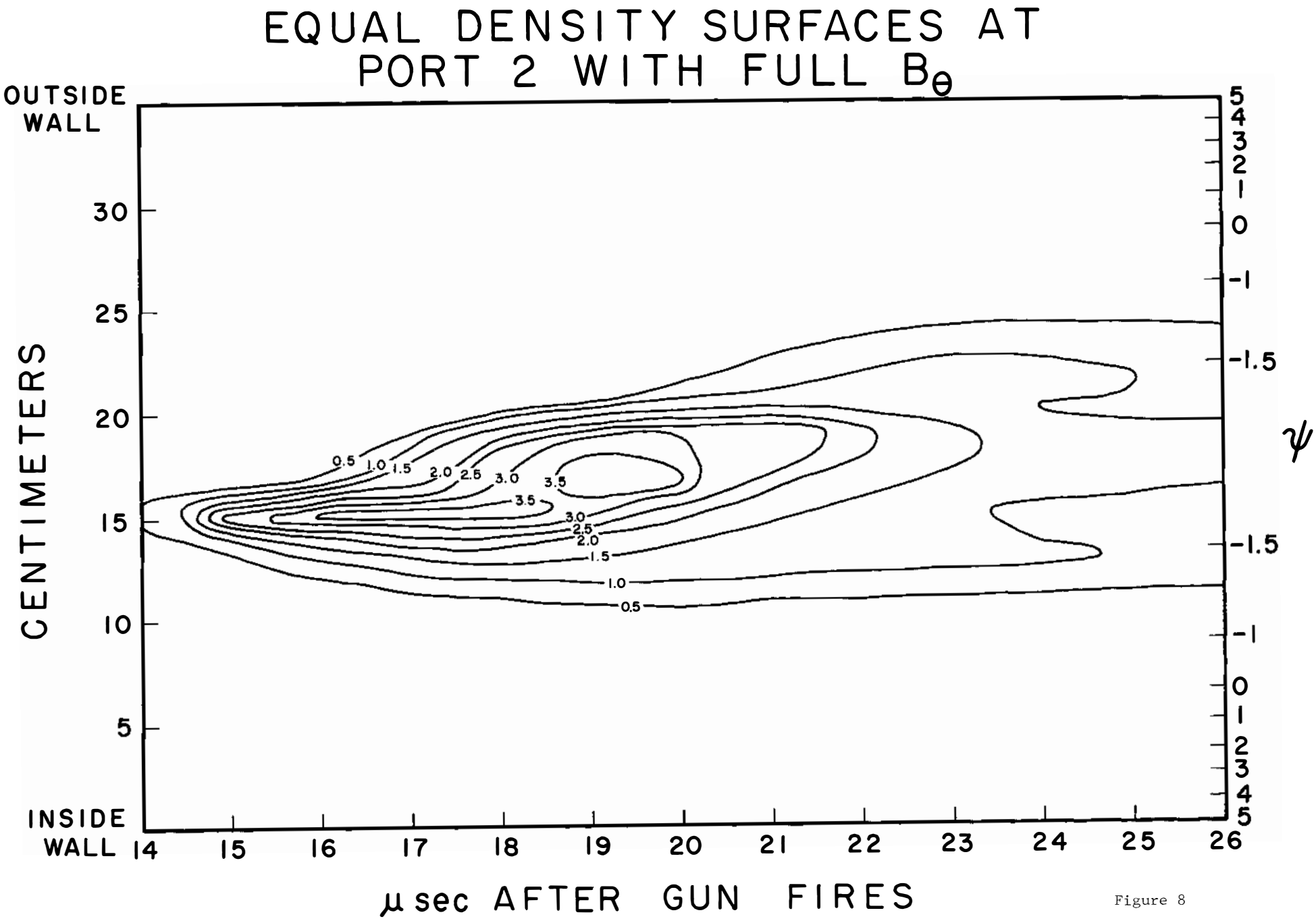
EQUAL DENSITY SURFACES AT
PORT 2 WITH FULL B_θ
OUTSIDE WALL
INSIDE WALL
CENTIMETERS
30
25
20
15
10
5
0.5
1.0
1.5
2.0
2.5
3.0
3.5
3.5
3.0
2.5
2.0
1.5
1.0
0.5
14
15
16
17
18
19
20
21
22
23
24
25
26
μ sec AFTER GUN FIRES
5
4
3
2
1
0
-1
-1.5
-1.5
-1
0
1
2
3
4
5
ψ

Figure 8